

# Reaction-condition-controlled formation of secondary-building-units in three cadmium metal–organic frameworks with an orthogonal tetrakis(tetrazolate) ligand

Christina S. Collins<sup>a</sup>, Daofeng Sun<sup>a</sup>, Wei Liu<sup>b</sup>, Jing-Lin Zuo<sup>b</sup>, Hong-Cai Zhou<sup>a,\*</sup>

<sup>a</sup> Department of Chemistry and Biochemistry, Miami University, Oxford, OH 45056, USA

<sup>b</sup> Coordination Chemistry Institute, State Key Laboratory of Coordination Chemistry, Nanjing University, Nanjing 210093, China

## ARTICLE INFO

### Article history:

Received 22 January 2008

Received in revised form 17 April 2008

Accepted 17 April 2008

Available online 30 April 2008

### Keywords:

Metal–organic framework

Tetrazole

Cadmium

Solvothermal synthesis

## ABSTRACT

Three metal–organic frameworks (MOFs) have been isolated using an orthogonal tetrakis(tetrazolate) ligand, ttbf (the tetra-anion of 2,2',7,7'-tetrakis(2*H*-tetrazol-5-yl)-9,9'-spirobi[fluorene], H<sub>4</sub>ttbf). These three MOFs were constructed using only (ttbf)<sup>4-</sup> and Cd<sup>2+</sup> by changing metal:ligand ratio, solvent, and source of anions. MOF **3** contains a very rare square–planar Cd<sub>4</sub> cluster bridged by a μ<sub>4</sub>-Cl atom. MOFs **1** and **3** have saturated metal centers prior to drying and do not thermally decompose until 315 °C. MOF **2**, however, has an unsaturated metal center prior to drying and its thermal-decomposition temperature is around 250 °C.

© 2008 Elsevier B.V. All rights reserved.

## 1. Introduction

There are numerous potential applications of metal–organic frameworks (MOFs) [1–7]. Controlled synthesis into “designed” 3D supramolecular structures remains an elusive goal [8–11]. Herein we demonstrate how to control the assembly of some MOFs with a tetrakis(tetrazolate) ligand by tuning three conditions: metal:ligand ratio, solvent, and source of anions.

Carboxylate ligands have been used for the construction of MOFs since the mid-1990s because they allow for a variety of structural motifs, and frequently provide good stability and permanent porosity [12–24]. Tetrazole ligands, on the other hand, have been used for medicinal purposes as far back as 1949 [25–30]. They have been used as analogs to carboxylic acids in synthesis [11,28–31] because of their low p*K*<sub>A</sub> (~4), and have even been examined via computational methods [25]. They have only become an interesting aspect of MOF chemistry, however, in the last 3–5 years [10,11,32–41]. The work herein also confirms the success of substituting carboxylic acids with tetrakis(tetrazolate) ligands in the synthesis of MOFs.

## 2. Experimental

### 2.1. Materials and methods

All commercially available chemicals were used without further purification. Elemental analyses (C, H, and N) were conducted by

Canadian Microanalytical Service, Ltd. Thermal gravimetric analyses were performed under N<sub>2</sub> on a PerkinElmer Delta Series TGA 7 instrument. Gas sorption measurements for N<sub>2</sub> were performed at 77 K on a Beckman–Coulter SA 3100 surface analyzer. Infrared absorption spectra were obtained using a PerkinElmer Spectrum One FT-IR with a universal diamond ATR sampling accessory in the 650–4000 cm<sup>-1</sup> region. Solution NMR data were collected on a Bruker 200 MHz spectrometer. Luminescence (excitation and emission) spectra for the solid samples were obtained with an AMINCO Bowman Series 2 luminescence spectrophotometer.

### 2.2. Synthesis of 2,2',7,7'-tetrakis(2*H*-tetrazol-5-yl)-9,9'-spirobi[fluorene] (H<sub>4</sub>ttbf)

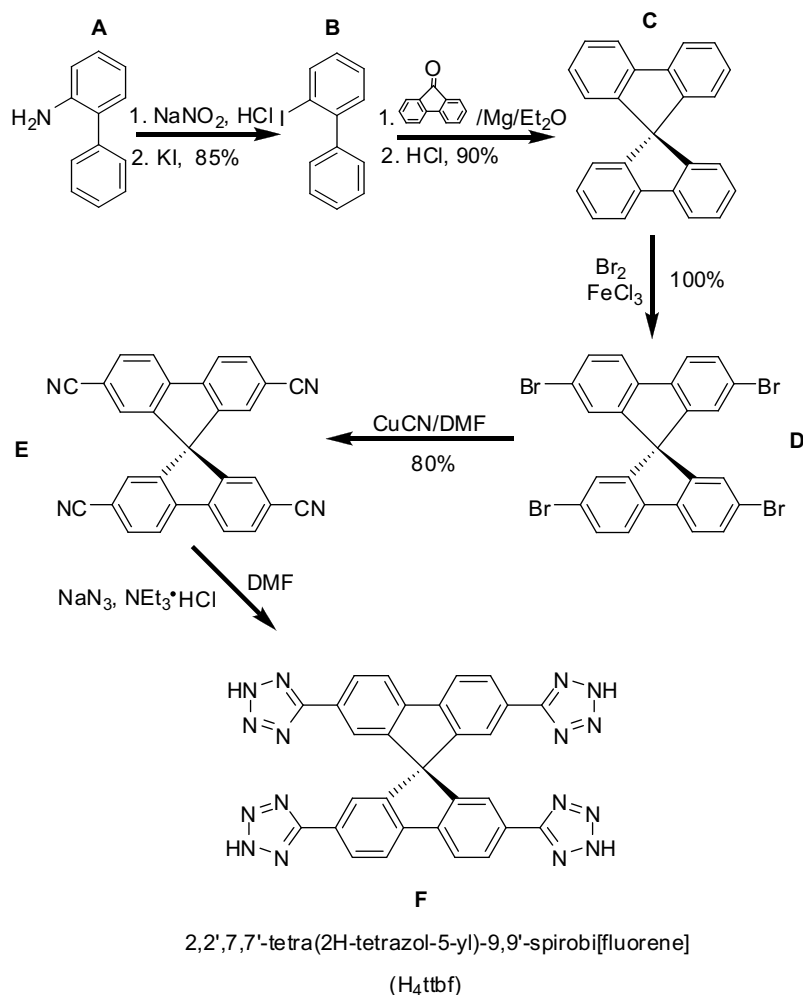
By following Scheme 1, compound E (3.80 g, 9 mmol) was dissolved in 150 mL dried DMF and NEt<sub>3</sub>·HCl (6.80 g, 50 mmol) and NaN<sub>3</sub> (3.30 g, 50 mmol) were added under N<sub>2</sub> and refluxed for 20 h. After filtration, the solution was acidified with diluted HCl to a fine white precipitate. The solid was filtered again and washed with water several times. Yield: 3.23 g (85%). <sup>1</sup>H NMR (DMSO, 200 MHz) δ 8.5 (d, 4 H), 8.3 (d, 4 H), 7.4 (s, 4H).

### 2.3. Synthesis of metal–organic frameworks

#### 2.3.1. Cd<sub>2</sub>(ttbf)(CH<sub>3</sub>OH)<sub>5</sub>·3H<sub>2</sub>O (**1**)

A mixture of Cd(NO<sub>3</sub>)<sub>2</sub>·4H<sub>2</sub>O (10.0 mg, 32.4 μmol) and H<sub>4</sub>ttbf (10.0 mg, 17.1 μmol) in MeOH (2 mL) was sealed in a Pyrex tube under vacuum. The tube was heated at 115 °C for 2 days, and then cooled to room temperature at a rate of 0.1 °C/min. The resulting

\* Corresponding author. Tel.: +1 513 529 8091; fax: +1 513 529 0452.  
E-mail address: [zhouh@muohio.edu](mailto:zhouh@muohio.edu) (H.-C. Zhou).

Scheme 1. Synthetic scheme of H<sub>4</sub>ttbf.

colorless crystals were washed with MeOH to give pure compound **1**; the crystals were also suitable for single-crystal X-ray diffraction studies. Yield: 5.9 mg (34%). Anal. Calc. for C<sub>34</sub>H<sub>38</sub>N<sub>16</sub>O<sub>8</sub>Cd<sub>2</sub>: C, 39.89; H, 3.75; N, 21.90. Found: C, 39.97; H, 3.20; N, 20.15%.  $\nu_{\max}(\text{-neat})/\text{cm}^{-1}$  1615m, 1520w, 1446m, 1420s, 1257w, 950m, 829s, 762s, 742vs.

### 2.3.2. Cd<sub>2</sub>O(H<sub>2</sub>ttbf)(C<sub>3</sub>H<sub>7</sub>NO)<sub>2</sub>·CH<sub>3</sub>OH·4H<sub>2</sub>O (**2**)

A mixture of Cd(NO<sub>3</sub>)<sub>2</sub>·4H<sub>2</sub>O (10.0 mg, 32.4 μmol) and H<sub>4</sub>ttbf (20.0 mg, 34.2 μmol) in a 1:1 DMF/MeOH (2 mL) mixture was sealed in a Pyrex tube under vacuum. The tube was heated at 80 °C for 2 days, and then cooled to room temperature at a rate of 0.1 °C/min. The resulting small colorless crystals were washed with DMF and then MeOH to give pure compound **2**; the crystals were also suitable for single-crystal X-ray diffraction studies. Yield 6.7 mg (18%). Anal. Calc. for C<sub>36</sub>H<sub>42</sub>N<sub>18</sub>O<sub>8</sub>Cd<sub>2</sub>: C, 40.05; H, 3.92; N, 23.35. Found: C, 40.21; H, 3.55; N, 22.79%.  $\nu_{\max}(\text{neat})/\text{cm}^{-1}$  1616w, 1520w, 1447m, 1419s, 1232w, 951w, 828s, 761s, 742vs.

### 2.3.3. Cd<sub>2</sub>Cl(Httbf)(C<sub>3</sub>H<sub>7</sub>NO)(H<sub>2</sub>O)·CH<sub>3</sub>OH·3H<sub>2</sub>O (**3**)

Three drops of 1.0 M HCl was added to a mixture of Cd(NO<sub>3</sub>)<sub>2</sub>·4H<sub>2</sub>O (10.0 mg, 34.2 μmol) and H<sub>4</sub>ttbf (20.0 mg, 34.2 μmol) in a 1:1 DMF/MeOH (2 mL) mixture and the reaction mixture was sealed in a Pyrex tube under vacuum. The tube was heated at 80 °C for 2 days, and then cooled to room temperature

at a rate of 0.1 °C/min. The resulting large colorless crystals were washed with DMF and then MeOH to give pure compound **3**; the crystals were also suitable for single-crystal X-ray diffraction studies. Anal. Calc. for C<sub>33</sub>H<sub>32</sub>N<sub>17</sub>O<sub>6</sub>ClCd<sub>2</sub>: C, 38.74; H, 3.15; N, 23.28. Found: C, 36.29; H, 3.18; N, 21.62%. Yield: 14.0 mg (40%).  $\nu_{\max}(\text{-neat})/\text{cm}^{-1}$  2923m, 2851w, 1615vw, 1457m, 1420s, 1232w, 1180w, 957w, 826s, 760s, 743vs.

## 2.4. Crystallographic studies

Single-crystal X-ray diffraction studies for **1** and **2** were performed on a Bruker Apex D8 CCD diffractometer equipped with a fine-focus sealed-tube X-ray source [graphite monochromated MoK<sub>α</sub> radiation ( $\lambda = 0.71073 \text{ \AA}$ )] operating at 40 kV and 40 mA. Crystals of **1** and **2** were mounted on glass fibers and maintained under a stream of N<sub>2</sub> at 213 K. The structure of **3** was determined using a specially configured diffractometer based on the Bruker-Nonius X8 Proteum using focused CuK<sub>α</sub> radiation ( $\lambda = 1.54178 \text{ \AA}$ ). Crystals of **3** were mounted on glass fibers and maintained under a stream of N<sub>2</sub> at 90 K. Raw data collection and cell refinement were done using SMART; data reduction was performed using SAINT+ and corrected for Lorentz and polarization effects [42]. Structures were solved by direct methods using SHELXTL and were refined by full-matrix least-squares on  $F^2$  using SHELX-97 [43]. Non-hydrogen atoms were refined with anisotropic displacement parameters during the final cycles. Hydrogen atoms were placed

in calculated positions with isotropic displacement parameters set to  $1.2 \times U_{eq}$  of the attached atom.

### 3. Results and discussion

#### 3.1. Structural description of **1**

The solvothermal reaction between  $\text{Cd}(\text{NO}_3)_2 \cdot 4\text{H}_2\text{O}$  and  $\text{H}_4\text{ttbf}$  in a 1:1 ratio carried out in methanol yields colorless block crystals of  $\text{Cd}_2(\text{ttbf})(\text{CH}_3\text{OH})_5 \cdot 3\text{H}_2\text{O}$  (**1**) which are suitable for X-ray diffraction studies. Crystal structure and refinement data are summarized in Table 1. Single-crystal diffraction analysis shows that **1** crystallizes in space group  $P2_1/c$  and has two non-identical six-coordinate cadmium atoms that make up a dinuclear SBU (secondary building unit, Fig. 1).

$\text{Cd}(1)$  is coordinated to four nitrogen atoms from four different ttbf ligands and two oxygen atoms from two MeOH molecules in a distorted octahedral geometry with Cd–N distances of 2.295–2.415 Å;  $\text{Cd}(2)$  is coordinated to three nitrogen atoms from three different ttbf ligands and three oxygen atoms from three MeOH molecules in a distorted octahedral geometry with Cd–N distances of 2.293–2.329 Å.

All tetrazole ( $-\text{CN}_4$ ) groups of ttbf are deprotonated during the solvothermal reaction, which is in agreement with the infrared data: no N–H stretch characteristic of secondary amines is visible around  $3400 \text{ cm}^{-1}$ . Every ttbf connects four SBUs to generate a 3D non-interpenetrating (4,4)-connected net with the cooperite (PtS) topology (Fig. 2) [44].

Framework **1** possesses pores having atom-center-to-atom-center dimensions of  $10.893 \times 14.180 \text{ Å}$  that are occupied by coordinated MeOH and free water molecules. A void volume after guest removal of 45.2%, or  $2052.4 \text{ Å}^3$  per  $4544.0 \text{ Å}^3$ , is calculated using the SOLV routine of the PLATON program [45].

#### 3.2. Structural description of **2**

The solvothermal reaction between  $\text{Cd}(\text{NO}_3)_2 \cdot 4\text{H}_2\text{O}$  and  $\text{H}_4\text{ttbf}$  in a 1:2 ratio carried out in MeOH and *N,N*-dimethylformamide (DMF) yields colorless block crystals of  $\text{Cd}_2\text{O}(\text{H}_2\text{ttbf})(\text{C}_3\text{H}_7\text{NO})_2 \cdot \text{CH}_3\text{OH} \cdot 4\text{H}_2\text{O}$  (**2**) that are suitable for X-ray diffraction studies. Crystal structure and refinement data are summarized in Table 1. Single-crystal diffraction analysis shows that **2** crystallizes in space group  $P\bar{1}$  and has a novel  $C_i$  symmetric cadmium tetranuclear SBU with Cd...Cd edge distances of 3.811 and 3.656 Å (Fig. 3).

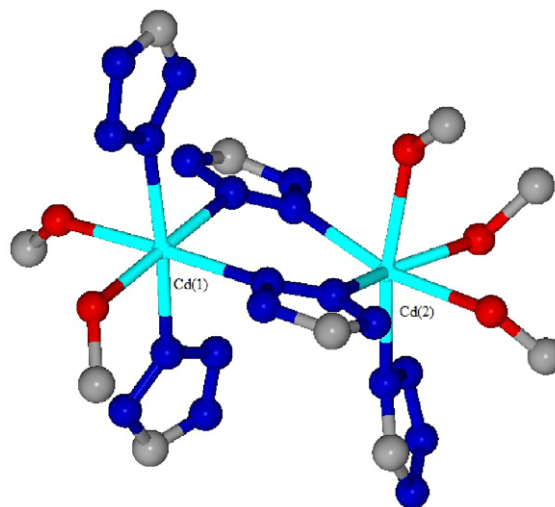


Fig. 1. The coordination environment of cadmium in **1**.

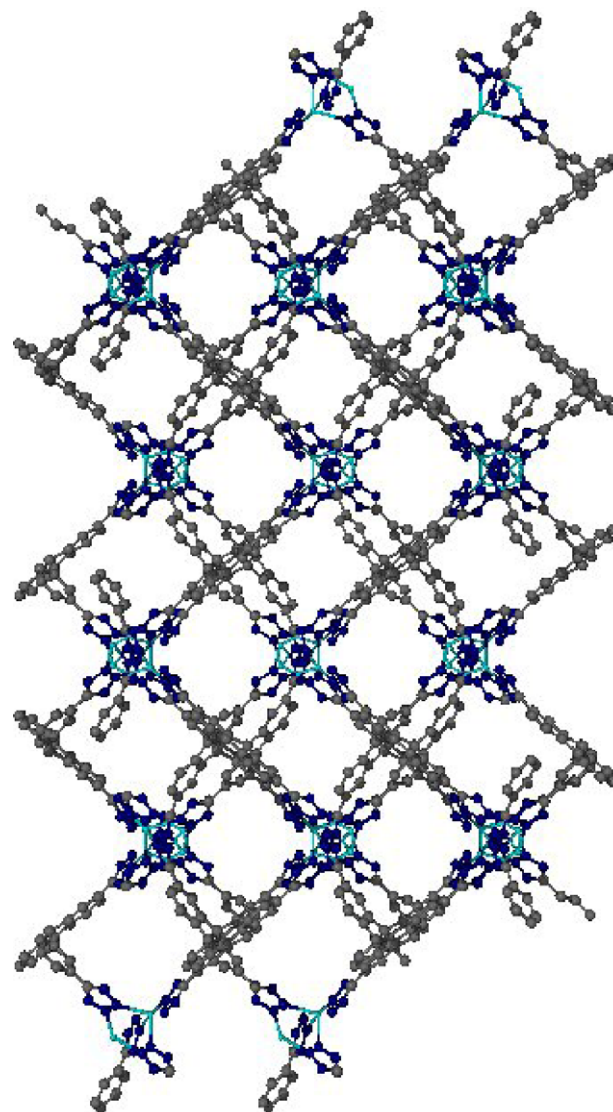


Fig. 2. View of the 3D net along *c*-axis in **1**. Solvent molecules have been omitted for clarity.

**Table 1**  
Crystal and structure refinement data for **1**, **2** and **3**

	<b>1</b>	<b>2</b>	<b>3</b>
Chemical formula	$\text{C}_{37}\text{Cd}_2\text{H}_{46}\text{N}_{16}\text{O}_9$	$\text{C}_{31}\text{Cd}_2\text{H}_{22}\text{N}_{16}\text{O}_3$	$\text{C}_{64}\text{Cd}_4\text{C}_4\text{H}_{40}\text{N}_{34}\text{O}_4$
Fw ( $\text{g mol}^{-1}$ )	1083.70	891.45	1834.35
Space group	$P2_1/c$	$P\bar{1}$	$Cccm$
<i>T</i> (K)	293(2)	213(2)	90(2)
$\lambda$ (Å)	0.71073	0.71073	1.54178
<i>a</i> (Å)	10.893(10)	12.1055(16)	19.738(2)
<i>b</i> (Å)	23.553(15)	14.7234(19)	21.866(2)
<i>c</i> (Å)	18.162(15)	15.2615(19)	26.821(2)
$\alpha$ (°)	90.00	66.228(2)	90.00
$\beta$ (°)	102.80(3)	66.188(2)	90.00
$\gamma$ (°)	90.00	83.164(3)	90.00
<i>V</i> (Å <sup>3</sup> )	4544(6)	2309.6(5)	11575.7(18)
<i>z</i>	4	2	4
$\mu$ ( $\text{mm}^{-1}$ )	1.004	0.965	6.397
$R_1^a, wR_2^b$ (%)	0.073, 0.20	0.084, 0.24	0.11, 0.31
GOF ( $F^2$ )	1.073	0.911	1.089

<sup>a</sup>  $R_1 = \sum |F_o| - |F_c| / \sum |F_o|$ .

<sup>b</sup>  $wR_2 = \{ \sum [w(F_o^2 - F_c^2)^2] / \sum [w(F_o^2)^2] \}^{1/2}$ ;  $w = 1 / [ \sigma^2(F_o^2) + (aP)^2 + bP ]$ ,  $P = [ \max(F_o^2 \text{ or } 0) + 2(F_c^2) ] / 3$ .



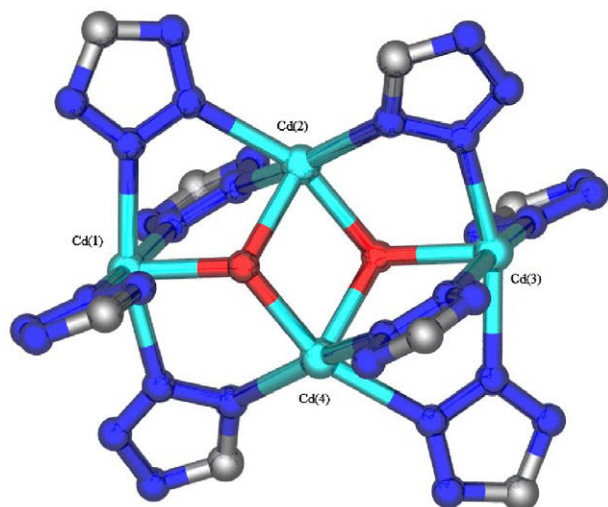


Fig. 3. View of the binuclear zinc SBU in **2**. Solvent molecules on Cd(2) and Cd(4) have been omitted for clarity.

The two  $\mu_3$ -O atoms within the SBU seem to serve two purposes in the formation of **2**. As an anion source, it balances the charges caused by partially deprotonated ligands, and it bridges Cd(1) to Cd(2) and Cd(3) and likewise, Cd(3) to Cd(2) and Cd(4). Each ttbf ligand connects three tetranuclear cadmium SBUs to generate a 3D non-interpenetrating (3,6)-connected net with the rutile ( $\text{TiO}_2$ ) topology [44] (Fig. 4).

The four cadmium atoms are not coordinatively identical: Cd(2) and Cd(4) have distorted octahedral geometries, Cd(1) and Cd(3) are unsaturated metal centers (UMCs) with square pyramidal geometries. The UMCs appear to have formed because of steric hin-

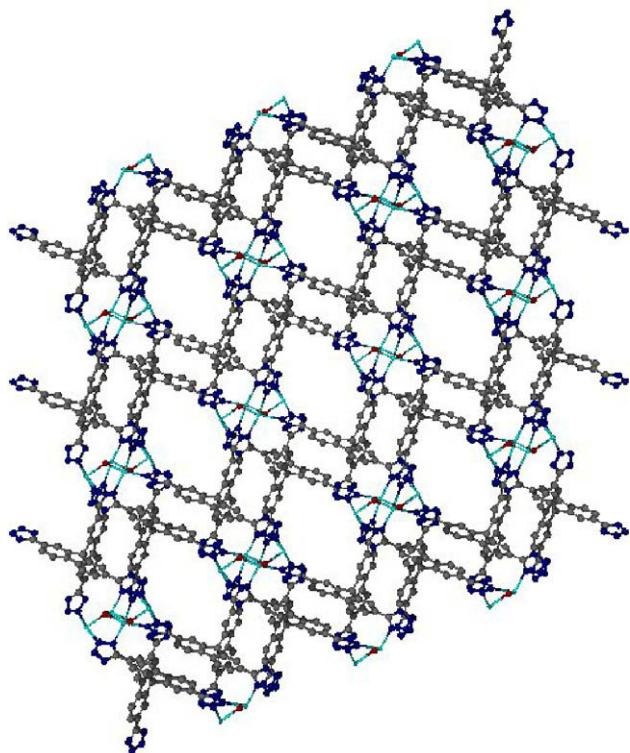


Fig. 4. View of the 3D net along *a*-axis in **2**. Solvent molecules have been omitted for clarity.

drance: they are not exposed to the channels, so they are not accessible by the bulky DMF ligand but may be accessible by smaller molecules. To the best of our knowledge, **2** is the first  $\text{Cd}^{2+}$  and tetrakis(tetrazolate) MOF with UMCs prior to desolvation.

Framework **2** possesses pores having atom-center-to-atom-center dimensions of  $8.854 \times 13.017 \text{ \AA}$  that are occupied by coordinated DMF and free MeOH and water molecules. A void volume after guest removal of 25.6%, or  $1165.2 \text{ \AA}^3$  per  $4544.0 \text{ \AA}^3$ , is calculated using PLATON [45].

### 3.3. Structural description of **3**

The solvothermal reaction between  $\text{Cd}(\text{NO}_3)_2 \cdot 4\text{H}_2\text{O}$  and  $\text{H}_4\text{ttbf}$  in a 1:2 ratio carried out in MeOH, DMF and 1.0 M hydrochloric acid (HCl) yields colorless block crystals of  $\text{Cd}_2\text{Cl}(\text{Httbf})(\text{C}_3\text{H}_7\text{NO})(\text{H}_2\text{O}) \cdot \text{CH}_3\text{OH} \cdot 3\text{H}_2\text{O}$  (**3**) which are suitable for X-ray diffraction studies. Crystal structure and refinement data are summarized in Table 1. Single-crystal diffraction analysis shows that **3** crystallizes in space group *Cccm* and has a  $\text{C}_2$  symmetric tetranuclear cadmium SBU (Fig. 5) with Cd–Cl distances of 2.701 and 2.876 Å which is nearly identical to the square planar  $\text{Mn}_4\text{Cl}$  cluster reported by Long and coworkers [40], and topologically resembles the  $\text{Co}_4\text{O}$  SBU previously reported [46]. In **3**, HCl is the source of the bridging chloro anion whose charge balances a charge caused by partial deprotonation of ligands. While all four cadmium atoms have distorted octahedral geometries, Cd(1 and 3) are coordinated to one DMF molecule, four ttbf ligands, and the  $\mu_4$ -Cl; Cd(2 and 4) are coordinated to one water molecule, four ttbf ligands, and the  $\mu_4$ -Cl.

A helical structure seen in **3** arises from SBUs aligned in the *z*-direction, with each successive SBU offset by  $45^\circ$ . Within each SBU there are four square-planar  $[\text{Cd}_4\text{Cl}]^{7+}$  units that are surrounded by eight tetrazolates to form a 3D non-interpenetrating binodal (4,8)-connected net with the fluorite ( $\text{CaF}_2$ ) topology (Fig. 6) [44].

Framework **3** possesses two types of pores, a smaller oval-shaped pore and a slightly larger rectangular pore having atom-center-to-atom-center dimensions of  $9.947 \times 10.757 \text{ \AA}$  and  $10.935 \times 14.475 \text{ \AA}$ , respectively, and are occupied with coordinated DMF and water molecules (Fig. 7). A void volume after guest removal of 75.9%, or  $3447.9 \text{ \AA}^3$  per  $4544.0 \text{ \AA}^3$ , is calculated using PLATON [45].

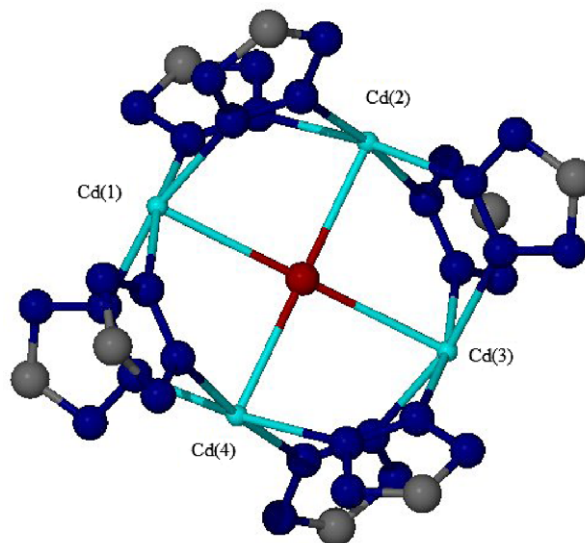


Fig. 5. View of the tetranuclear cadmium SBU in **3**. Solvent molecules have been omitted for clarity.

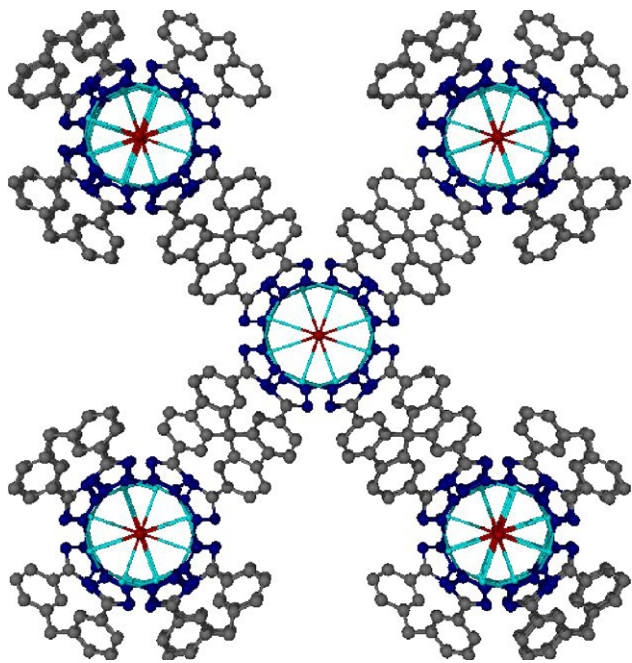


Fig. 6. View of the 3D net along *c*-axis in **3**. Solvent molecules have been omitted for clarity.

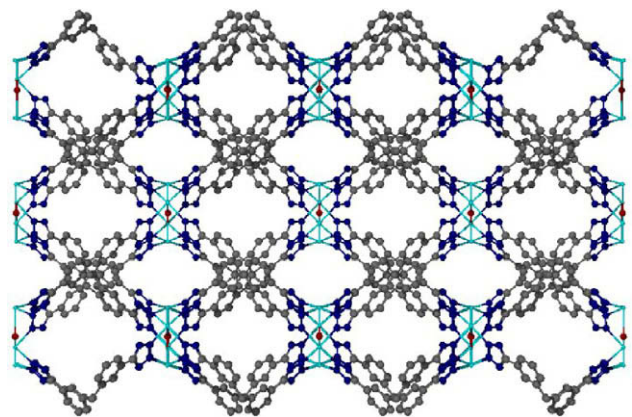


Fig. 7. View of the 3D net along *a*-axis in **3**. Solvent molecules have been omitted for clarity.

### 3.4. Thermogravimetric studies

As far as the thermal behavior of compounds **1–3** is concerned, the following can be emphasized:

(i) TGA (thermogravimetric analysis) shows that **1** has a two-step weight loss. The first weight loss (21.2%) from 50 to 190 °C corresponds to the loss of MeOH and solvate water molecules (calc. 21.0%). The second gradual weight loss (57.1%) from 190 to 315 °C corresponds to the decomposition of one ttbf ligand (calc. 56.8%).

(ii) TGA shows that **2** has a three-step weight loss. The first weight loss (9.54%) from 50 to 250 °C corresponds to the loss of MeOH and four free water molecules (calc. 9.68%). The second weight loss (14.16%) from 250 to 350 °C corresponds to the loss of two coordinated DMF molecules (calc. 13.59%). The final gradual weight loss (56.22%) from 350 to 650 °C corresponds to the decomposition of one ttbf ligand (calc. 54.34%).

(iii) TGA shows that **3** has a three-step weight loss. The first weight loss (9.72%) from 50 to 150 °C corresponds to the loss of MeOH and three free water molecules (calc. 8.42%). The second

weight loss (9.65%) from 150 to 315 °C corresponds to a coordinated water and DMF molecule (calc. 8.91%). The third gradual weight loss (57.01%) from 315 to 690 °C corresponds to the decomposition of one ttbf ligand (calc. 57.19%).

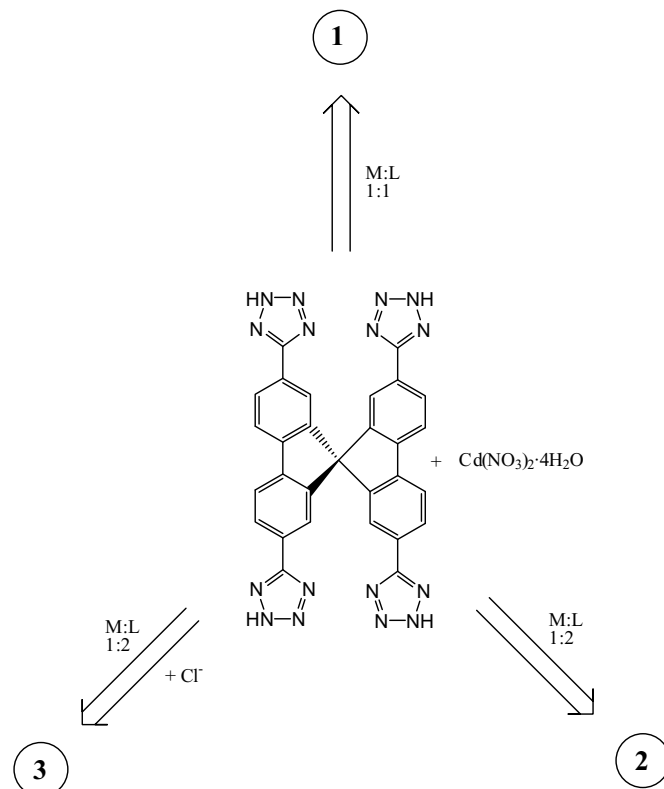
### 3.5. Secondary building units

It can be seen from this work that manipulating the metal:ligand ratio, solvent, and source of anions allows for the synthesis of very different frameworks while using the same cadmium salt and the ttbf ligand (Scheme 2).

Due to the various coordination modes the ligand allows and the numerous choices of SBUs (metal clusters), it can prove difficult to predict the final structure of the MOF. However, by tuning the conditions of the solvothermal reactions, a better grasp on assembly can be achieved (Scheme 2).

Consider the SBUs of **1**, **2**, and **3**. MOF **1** has a dinuclear SBU (Fig. 1), while **2** and **3** have tetranuclear SBUs (Figs. 3 and 5, respectively). There are two reasons for the varied SBU formation. Firstly, **1** is the only MOF with a single solvent used. The use of MeOH in the assembly of **1** increases the solubility of the metal salt:  $H_4ttbf$  is only slightly soluble in MeOH at room temperature. MOFs **2** and **3**, however, use mixed solvent systems to control the solubility of the ligand: the addition of DMF to MeOH increases the solubility of the ligand. With more ligand dissolved, there is more available ligand to bind the metal. Secondly, the metal:ligand ratio is decreased for the assembly of **2** and **3**. There is twice as much ligand available in the assembly reactions of **2** and **3** than in **1**. The excess of ligand allows the metal coordination sphere to be satisfied primarily by ligand donor atoms instead of supplementary solvent molecules. Given these two factors, it is clear why **2** and **3** have higher nuclearity SBUs than **1**.

Also of note are the two sources of auxiliary ligands that were manipulated in the synthetic methods. In **1**, only MeOH is available



Scheme 2. Solvothermal reaction conditions for **1**, **2**, and **3**.

for coordination to the cadmium metals. In **2** and **3**, however, there is a 1:1 mixture of DMF:MeOH; the solvents are now in competition for coordination and DMF is the better ligand. In **2**, therefore, DMF coordinates to the cadmium metals and MeOH is conserved in the lattice. MOF **2** requires a source of anions to balance the charge of partial deprotonation of the ligand, so  $O^{2-}$  is the bridging ligand in **2**. In **3**, however, there is another source of anions present to balance the positive charge from the partially deprotonated ligand – HCl – that enables  $Cl^-$  to bridge the metals in **3**.

In addition, the pH value during the assembly procedure may play a key role in determine whether the ligand is completely deprotonated, as in **1**, or partially deprotonated, as in **2** and **3**.

Even with a single metal source and one ligand, three different MOFs were obtained when reaction conditions changed.

### 3.6. Gas sorption

Gas sorption measurements for  $N_2$  were performed on **1**, **2**, and **3**. As-synthesized samples **2** and **3** were exchanged overnight with methanol to remove DMF, washed with MeOH, and dried under vacuum at 140 °C. IR confirms the disappearance of DMF from **2** and **3**, as the carbonyl stretch characteristic of a tertiary amide at  $1640\text{ cm}^{-1}$  is absent. MOF **1** was directly dried under a dynamic vacuum since no DMF was involved in the preparation.  $N_2$  sorption at 77 K, however, shows that **1**, **2**, and **3** have no permanent porosity. Even though **2** has unsaturated metal sites in the form of square pyramidal geometries that should enable a high affinity to  $H_2$  molecules [40,41,46–48], there is little accessibility to these sites.

### 3.7. Photoluminescence

Photoluminescence measurements for **1**, **2**, and **3** show that these MOFs exhibit strong luminescence at  $\lambda_{\text{max}} = 409, 409,$  and  $410\text{ nm}$ , respectively, upon excitation at 362, 364, and 366 nm, respectively, as shown in Fig. 8. The emissions of MOFs **1–3** can be assigned to an intra-ligand  $\pi \rightarrow \pi^*$  transition, although a sizable blue-shift (approx. 79 nm) is observed in the MOFs. Emission by **1–3** is considerably more intense than that of the free ligand. This may be explained in terms of ligand rigidity: in solution at room temperature,  $H_4\text{ttbf}$  is more flexible than the  $\text{ttbf}$  ligand within an MOF; this rigidity of the coordinated ligand effectively reduces the loss of energy, thereby increasing fluorescent efficiency [49].

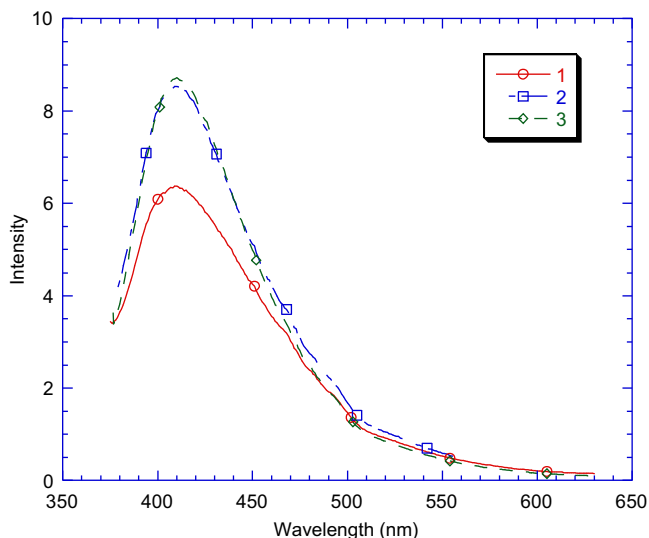


Fig. 8. Emission spectra for **1–3**.

## 4. Conclusions

Three metal–organic frameworks based on a tetrakis(tetrazolate) ligand have been successfully isolated through solvothermal reactions. Finely tuning each solvothermal reaction condition has helped us to better understand the formation of SBUs and hopefully predict MOF assembly of similar reactions in the future. With the control of reaction conditions, we believe that in an assembly procedure the behavior of any ligand that encourages differing coordination modes can be better comprehended. However, the “prediction” or “design” of a MOF remains largely a challenge.

## Acknowledgements

This work was supported by the National Science Foundation (Grant CHE-0449634) and Miami University. H.-C.Z. also acknowledges Research Corporation for a Research Innovation Award and a Cottrell Scholar Award. The Bruker Apex D8 CCD diffractometer was used in cooperation with the Miami University Department of Geology and funded by NSF Grant EAR-0003201. The Bruker-Nonius X8 Proteum diffractometer was used in cooperation with Dr. Sean Parkin and the University of Kentucky Department of Chemistry and funded by NSF Grant CHE-0449634. We also thank David Collins and Dr. Xi-Sen Wang for discussion.

## Appendix A. Supporting information

Crystallographic data for the structural analysis have been deposited with the Cambridge Crystallographic Data Centre, CCDC Nos. 627933–627935 for **1–3**, respectively. Copies of this information may be obtained free of charge from the CCDC, 12 Union Road, Cambridge, CB2 1EZ, UK (fax: +44 1223 336 033; e-mail: deposit@ccdc.cam.ac.uk or <http://www.ccdc.cam.ac.uk>).

## References

- [1] M. Eddaoudi, J. Kim, D.T. Vodak, A. Sudik, J. Wachter, M. O’Keeffe, O.M. Yaghi, Proc. Natl. Acad. Sci. USA 99 (2002) 4900.
- [2] M. Eddaoudi, D.B. Moler, H. Li, B. Chen, T.M. Reineke, M. O’Keeffe, O.M. Yaghi, Acc. Chem. Res. 34 (2001) 319.
- [3] A. Firouzi, D. Kumar, L.M. Bull, T. Besier, P. Sieger, Q. Huo, S.A. Walker, J.A. Zasadzinski, C. Glinka, J. Nicol, Science 267 (1995) 1138.
- [4] O. Kahn, Acc. Chem. Res. 33 (2000) 647.
- [5] S. Kitagawa, R. Kitaura, S.-i. Noro, Angew. Chem. Int. Ed. 43 (2004) 2334.
- [6] B. Moulton, M.J. Zaworotko, Chem. Rev. 101 (2001) 1629.
- [7] O.M. Yaghi, H. Li, C. Davis, D. Richardson, T.L. Groy, Acc. Chem. Res. 31 (1998) 474.
- [8] P.-K. Chen, Y.-X. Che, J.-M. Zheng, Inorg. Chem. Commun. 10 (2007) 187.
- [9] J. Kim, B. Chen, T.M. Reineke, H. Li, M. Eddaoudi, D.B. Moler, M. O’Keeffe, O.M. Yaghi, J. Am. Chem. Soc. 123 (2001) 8239.
- [10] C. Jiang, Z. Yu, S. Wang, C. Jiao, J. Li, Z. Wang, Y. Cui, Eur. J. Inorg. Chem. (2004) 3662.
- [11] J.-R. Li, X.-H. Bu, G.-C. Jia, S.R. Batten, J. Mol. Struct. 828 (2007) 142.
- [12] D. Bradshaw, T.J. Prior, E.J. Cussen, J.B. Claridge, M.J. Rosseinsky, J. Am. Chem. Soc. 126 (2004) 6106.
- [13] H.K. Chae, D.Y. Siberio-Pérez, J. Kim, Y. Go, M. Eddaoudi, A.J. Matzger, M. O’Keeffe, O.M. Yaghi, Nature 427 (2004) 523.
- [14] B. Chen, M. Eddaoudi, S.T. Hyde, M. O’Keeffe, O.M. Yaghi, Science 291 (2001) 1021.
- [15] S.S.-Y. Chui, S.M.-F. Lo, J.P.H. Charmant, A.G. Orpen, I.D. Williams, Science 19 (1999) 1148.
- [16] Q.-R. Fang, G.-S. Zhu, M. Xue, J.-Y. Sun, S.-L. Qiu, Dalton Trans. (2006) 2399.
- [17] C.J. Kepert, T.J. Prior, M.J. Rosseinsky, J. Am. Chem. Soc. 124 (2000) 5158.
- [18] J.-H. Liao, P.-W. Wu, W.-C. Huang, Crystal Growth Des. 6 (2006) 1062.
- [19] T.J. Prior, M.J. Rosseinsky, Inorg. Chem. 42 (2003) 1564.
- [20] D. Sun, Y. Ke, D.J. Collins, G.A. Lorigan, H.-C. Zhou, Inorg. Chem. 46 (2007) 2725.
- [21] D. Sun, S. Ma, Y. Ke, D.J. Collins, H.-C. Zhou, J. Am. Chem. Soc. 128 (2006) 3896.
- [22] D. Sun, S. Ma, Y. Ke, T.M. Petersen, H.-C. Zhou, Chem. Commun. (2005) 2663.
- [23] O.M. Yaghi, H. Li, T.L. Groy, J. Am. Chem. Soc. 118 (1996) 9096.
- [24] C. Livage, N. Guillou, J. Marrot, G. Férey, Chem. Mater. 13 (2001) 4387.
- [25] A. Gomez-Zavaglia, I.D. Reva, L. Frija, M.L.S. Cristiano, R. Fausto, J. Photochem. Photobiol. A 180 (2006) 175.
- [26] US Patent, 2470084, 1949.
- [27] T. Mavromoustakos, A. Kolocouris, M. Zervou, P. Roumelioti, J. Matsoukas, R. Weisemann, J. Med. Chem. 42 (1999) 1714.

- [28] R.J. Herr, J. Bioorg. Med. Chem. 10 (2002) 3379.
- [29] Y. Tamura, F. Watanabe, T. Nakatani, K. Yasui, M. Fuji, T. Komurasaki, H. Tsuzuki, R. Maekawa, T. Yoshioka, K. Kawada, K. Sugita, M. Ohtani, J. Med. Chem. 41 (1998) 640.
- [30] A.F. Tominey, P.H. Docherty, G.M. Rosair, R. Quenardelle, A. Kraft, Org. Lett. 8 (2006) 1279.
- [31] T.-T. Luo, H.-L. Tsai, S.-L. Yang, Y.-H. Liu, R.D. Yadav, C.-C. Su, C.-H. Ueng, L.-G. Lin, K.-L. Lu, Angew. Chem. Int. Ed. 44 (2005) 6063.
- [32] A. Absmeier, M. Bartel, C. Carbonera, G.N.L. Jameson, P. Weinberger, A. Caneschi, K. Mereiter, J.-F. Letard, W. Linert, Chem. Eur. J. 12 (2006) 2235.
- [33] M. Dincă, A.F. Yu, J. Long, J. Am. Chem. Soc. 128 (2006) 8904.
- [34] X. He, C.-Z. Lu, D.-Q. Yuan, Inorg. Chem. 45 (2006) 5760.
- [35] A.V. Khripun, V.Y. Kukushkin, G.I. Koldobskii, M. Haukka, Inorg. Chem. Commun. 10 (2007) 250.
- [36] Z.-R. Qu, H. Zhao, X.-S. Wang, Y.-H. Li, Y.-M. Song, Y.-J. Liu, Q. Ye, R.-G. Xiong, B.F. Abrahams, Z.-L. Xue, X.-Z. You, Inorg. Chem. 42 (2003) 7710.
- [37] A. Rodriguez-Dieguez, E. Colacio, Chem. Commun. (2006) 4140.
- [38] J. Tao, Z.-J. Ma, R.-B. Huang, L.-S. Zheng, Inorg. Chem. 43 (2004) 6133.
- [39] X.-S. Wang, X.-F. Huang, R.-G. Xiong, Chin. J. Inorg. Chem. 21 (2005) 1020.
- [40] M. Dincă, A. Dailly, Y. Liu, C.M. Brown, D.A. Neumann, J. Long, J. Am. Chem. Soc. 128 (2006) 16876.
- [41] M. Dincă, W.S. Han, Y. Liu, A. Dailly, C.M. Brown, J.R. Long, Angew. Chem. Int. Ed. 46 (2007) 1419.
- [42] SAINT+, version 6.22; Bruker Analytical X-ray Systems, Inc., Madison, WI, 2001.
- [43] G.M. Sheldrick, SHELX-97, Bruker Analytical X-ray Systems, Inc., Madison, WI, 1997.
- [44] M. O'Keeffe, M. Eddaoudi, H. Li, T. Reineke, O.M. Yaghi, J. Solid State Chem. 152 (2000) 3.
- [45] A.L. Spek, J. Appl. Crystallogr. 36 (2003) 7.
- [46] S. Ma, H.-C. Zhou, J. Am. Chem. Soc. 128 (2006) 11734.
- [47] S. Ma, D. Sun, M. Ambrogio, J.A. Fillinger, S. Parkin, H.-C. Zhou, J. Am. Chem. Soc. 129 (2007) 1858.
- [48] J.-P. Zhang, S. Horike, S. Kitagawa, Angew. Chem. Int. Ed. 46 (2007) 889.
- [49] L.-Z. Cai, W.-T. Chen, M.-S. Wang, G.-C. Guo, J.-S. Huang, Inorg. Chem. Commun. 7 (2004) 611.